

## Combination of high-resolution AFM with super-resolution Stochastic Optical Reconstruction Microscopy (STORM)

### Introduction

Since its development in 1986, atomic force microscopy (AFM) has become a versatile tool in various fields of application. As a surface imaging technique it is traditionally used in materials research. Here, it is possible to resolve structures in the nanometer range with further opportunity of the investigation of material properties like friction, stiffness or magnetic and electrical characteristics. Over the years the potential use of AFM in life sciences, e.g. biology, biophysics, biochemistry and medicine came to the fore [1][2]. On the one hand, AFM as imaging method allows obtaining images in high-resolution under controlled and even physiological conditions. On the other hand, AFM can be used as a force sensor to measure mechanical properties, like Young's Moduli, as well as specific interaction forces like adhesion, receptor-ligand recognition and cell-cell interactions. Especially in life science research it has to be pointed out that a combination of AFM with standard optical techniques like phase contrast microscopy and conventional fluorescence microscopy is more and more essential. A combination of both techniques opens a new world of applications, where the optics can be used as assistance as well as extension to AFM. The use of AFM together with advanced optical techniques like confocal laser scanning microscopy or TIRF microscopy is also very promising due to the better optical resolution and/or higher signal-to-background ratios of these techniques [3]. Of course, AFM and optical microscopy yield different kinds of information. While optical microscopy provides the opportunity of a specific fluorescence labeling of a structure, AFM detects the mechanical properties of the investigated samples. Down to the diffraction limit the optical and AFM image

can be overlaid and correlated perfectly. Nevertheless, such a correlation leaves room for interpretation due to the different resolution ranges of both techniques. While AFM provides a nanometer resolution the conventional optical resolution is limited to a few hundred nanometers. This gap in resolution can now be filled by recently developed super-resolution techniques like Stimulated Emission Depletion Microscopy (STED), Stochastic Optical Reconstruction Microscopy (STORM) or Photo-activated Localization Microscopy (PALM), which reach an optical resolution of tens of nanometer [4]. This technical note should demonstrate the combination of AFM and STORM in a way of the general technical explanation as well as the huge benefits of a combination of both techniques.

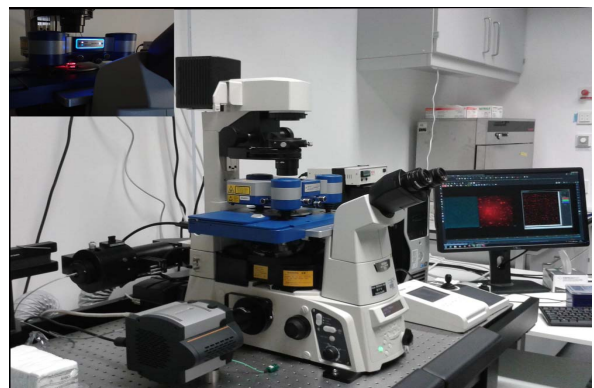


Figure 1: Nikon STORM setup in combination with JPK NanoWizard 3 AFM in the laboratory of Prof. Römer at BIOS, University of Freiburg, Germany.

### STORM

Ernst Abbe was the first to describe that the resolution of classical optical microscopy is fundamentally limited due to diffraction. He found that the resolution depends on the wavelength  $\lambda$  and on the numerical aperture of the optical system ( $NA = n * \sin \alpha$ , with the refractive index  $n$  and aperture angle):

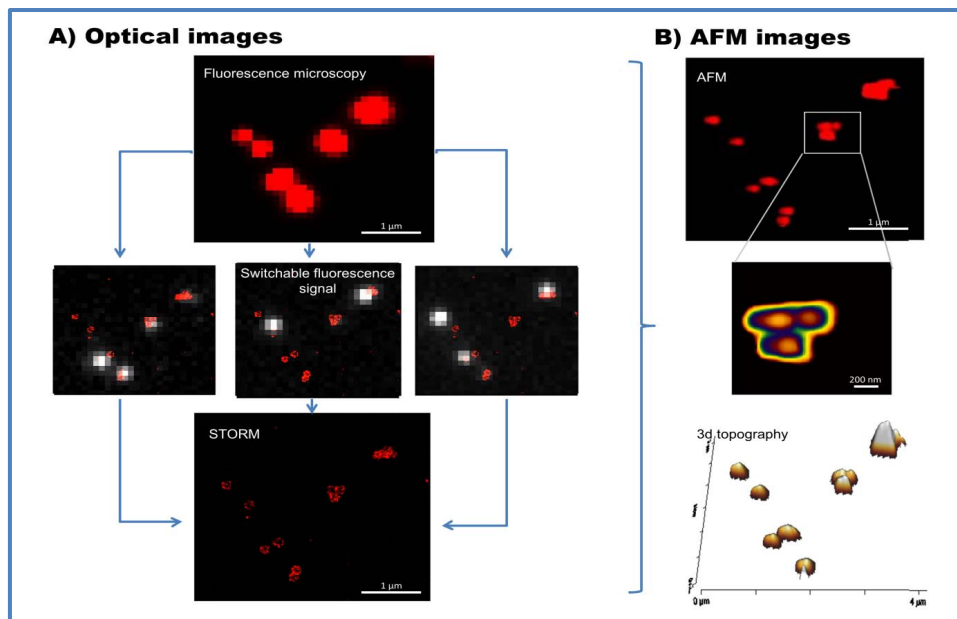


Figure 2: A) Schematic explanation of STORM principle on fluorescent labeled beads. Simultaneous excitation of all fluorophores results in a classical diffraction-limited image (upper image). By switching off most fluorophores and activating only a small subset, the position of the individual molecules can be determined with accuracy below the diffraction limit. Repeating this readout process for all molecules, i.e. recording thousands of images like the three displayed ones (white spots are the single molecule fluorescence signals), allows to measure all positions and to finally reconstruct the STORM image. 2B) AFM images are taken at the same position. Next to topography also mechanical information can be obtained in high resolution.

$$Resolution_{xy} = \frac{\lambda}{2NA} = \frac{\lambda}{2(n * \sin \alpha)}$$

The Abbe limit indicates that even with high-NA objectives structures separated less than ~200 nm in lateral dimension cannot be resolved [5][6]. In the last years, sophisticated approaches to surpass this fundamental barrier have been reported. One way to achieve super-resolution is based on single-molecule localization (PALM, FPALM and (d)STORM) [5][6][7]. The principle of these methods is to combine the high localization accuracy of single molecule imaging with photo-activation or –switching of individual fluorophores. Due to diffraction, images of point light sources such as single molecules are rather broad spots with an extent of a few hundred nanometers. However, the position of the molecule can be determined with nm-accuracy by using centroid fitting of the measured photon

distribution. For most scenarios, such a distribution can be sufficiently approximated by a Gaussian function. In a perfect microscope, i.e. low background level, highly sensitive EMCCD camera, etc., the localization error  $\sigma$  is mainly determined by  $s$ , the width of the point-spread function and  $N$ , the number of collected photons from the fluorescent molecule [8]:

$$\sigma \approx \frac{s}{\sqrt{N}}$$

In order to increase the localization precision it is necessary to use bright and photostable fluorophores together with a high power fluorescence excitation. Furthermore, precise single-molecule localization requires that the fluorescing molecules are well separated, i.e. by a distance above the diffraction limit. However, in typical samples, there are up to hundreds of fluorophores per diffraction limited volume. Therefore, it is necessary to adjust the concentration of actively

fluorescing molecules by mechanisms such as photo-activation or –switching. In STORM, this is realized by shifting the fluorophores into a dark state. For the actual readout, only a tiny fraction of the fluorophores is activated, either by spontaneous return from the dark-state or by inducing the return with an activation pulse of a short-wavelength laser. The fluorescence signals of the active fluorophores are recorded by using a high-power readout laser until the fluorophores either re-enter the dark state or photobleach. Then another subset of fluorophores is activated for the next readout. This process is repeated until the position of (almost) all fluorophores within the sample was measured. The super-resolved STORM image is reconstructed by combining all measured positions into one image. Figure 2 exemplifies the general approach for STORM and also demonstrates the increase in resolution. In diffraction limited fluorescence microscopy the beads appear as single spots. Also, signals from neighboring beads overlap and can therefore not be discriminated. For STORM thousands of individual images of switchable fluorophores are recorded to localize each molecule with nm-accuracy. As a result, it is possible to achieve a much higher optical resolution, so that single beads which are close together can be resolved (achievable resolution range of ~20-30 nm).

### Integration of AFM and STORM

For a perfect integration of AFM and STORM different requirements must be met.

a) Compatibility of AFM and STORM

In an optimal combination of AFM and optical techniques both methods do not disturb each other. Therefore, the JPK NanoWizard AFM is designed as a tip-scanning system. The sample remains fixed with respect to the optical microscope, while the AFM image can be recorded in parallel without moving the sample. The wavelength of the AFM laser is 880 nm, respectively 980 nm. This long wavelength in the IR

range prevents unwanted excitation of fluorophores used in STORM. Furthermore, IR light can be easily blocked in the fluorescence microscope, which is important to ensure a low background level for optical imaging. Typical STORM lasers show an excitation wavelength of e.g. 405nm, 488nm, 561nm and 647 nm. The AFM head is equipped with filters that block these wavelengths so that the detector is only sensitive for the AFM laser wavelength. These optimizations make a simultaneous, undisturbed optical and AFM measurement possible.

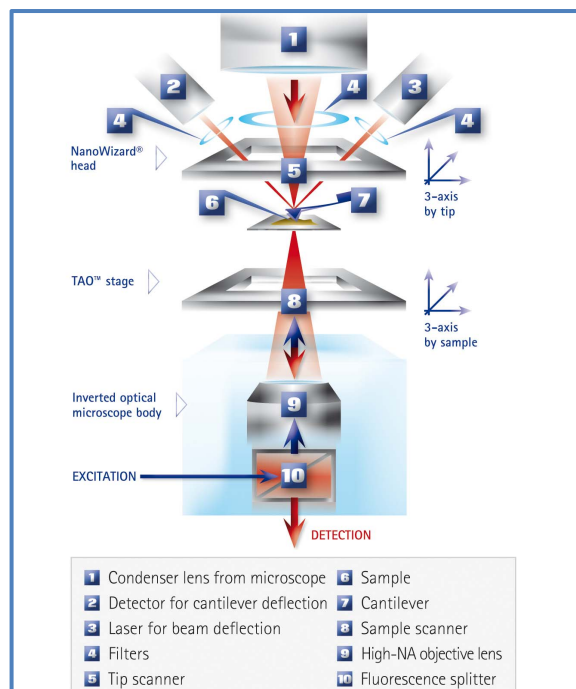


Figure 3: Sketch of a possible setup of an STORM-AFM combination. NanoWizard 3 AFM head is equipped with several filters. A TAO™ module and CoverslipHolder provides additional stability for the measurements.

b) Mechanical stability and drift compensation

It is needed that the setup demonstrates a high level of stability. Therefore, the setup must be equipped with vibration isolation. AFM is also quite sensitive to acoustic noise, which should be reduced as far as possible. Many super-resolution setups are configured with a focus drift correction system to maintain the correct focal plane. For better controlled positioning it is

also possible to use a piezo controlled stage. For advanced optical experiments JPK has developed the TAO™ module, which controls the sample position with closed-loop piezo accuracy in x, y, and z axis [10].



Figure 4: JPK TAO™ modules are recommended for advanced optical experiments and provide a closed-loop piezo sample positioning.

c) Camera

Furthermore, for a good STORM resolution it is necessary to use a sensitive low-light level EMCCD camera, e.g. from the Andor iXon series. For a better handling, the control of the Andor Camera is fully integrated in the JPK Instruments software. It is necessary to cool the EMCCD camera in order to achieve an optimal performance. Therefore, it is possible to use an internal fan or to use a water-cooling system. To reduce mechanical vibrations it is recommended to use a water-cooling system for an optimal AFM performance.

d) Sample holder

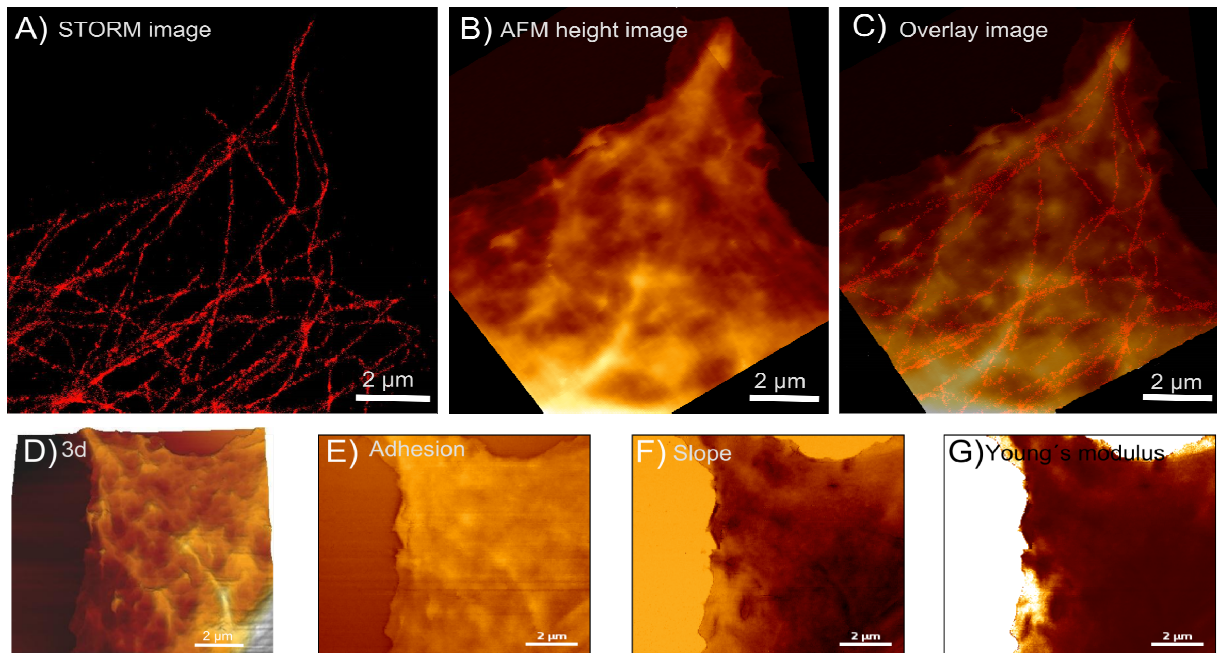
Typically 100x oil immersion objectives with excellent optical quality and a high numerical aperture (NA) are used for STORM. Such objectives are normally optimized for 170 µm thick coverslips. These thin glass slides tend to be mechanically instable, which makes them incompatible to high-resolution AFM measurements without special sample fixation. To achieve a sub-nanometer resolution with AFM in combination with the required coverslip the JPK CoverslipHolder™ and BioCell™ were designed. Both holders fix a coverslip in an optimum, high mechanical stable matter, while the Biocell™ furthermore provides a temperature control.



Figure 5: JPK CoverslipHolder™ (left) and BioCell™ (right)

e) Software – DirectOverlay™

To achieve a perfect combination of optics and AFM down to the molecular scale at the end, distortions must be prevented. Distortions mean that two images like optical and AFM images do not perfectly overlay. Reasons for distortions are errors like aberrations arising from the lenses and mirrors of the optical system, while the AFM is piezo controlled with accuracy down to the angstrom range. Nonlinear stretching, rotating and offsetting of optical images can be especially observed in normal optical microscopes. In a STORM setup with high optical characteristics distortions are much smaller. To achieve a perfect match of the optical and the AFM image it is necessary to correct the detected distortions. This is automatically done by the patented JPK DirectOverlay™ algorithm. Here, the AFM tip is placed at 25 different positions within the field of view and the AFM scan range. On each position an optical image is taken and used to evaluate and correct the distortions for the used optical setup. This provides an overlay of the optical and the AFM in maximum down to the molecular scale (for further information see application note: [“True integration of optical and atomic force microscopy”](#))



**Figure 6 A-C)** Combination of STORM and AFM on HeLa cells A) The microtubules were labeled with Alexa647 via immuno-fluorescence staining and measured with dSTORM. Individual microtubules and their distribution can be clearly resolved. B) AFM image on the same position was taken to get further information about the cell membrane surface texture (z-range: 400 nm). C) Overlay of AFM and STORM to get information about possible correlations of the optical and mechanical data.

**6 D-G)** Further AFM images to demonstrate the mechanical properties of the HeLa cell. D) 3D topography image (z-range: 400nm). E) Adhesion image (z-range: 300pN) shows the stickiness of the cell. F-G) Slope and Young's Modulus image show the elasticity of the investigated cell. While the slope image (z-range: 25 nN/μm) provides just the stiffness distributions via linear fitting of the extend curve, the Young's modulus image (z-range: 40 kPa) shows the calculated elasticity values by using the Hertz fit.

### Application example 1: labeled beads

As a first proof of concept experiment fluorescently labeled beads were measured. The bead preparation was performed similar to a protocol used in Huang et al. [20]. Coverslips were coated with poly-L-lysine and then incubated with a 0.1 mg/ml solution of unlabeled NeutrAvidin. NeutrAvidin is a deglycosylated version of avidin and demonstrates a high biotin binding affinity. Then, a suspension of biotin-functionalized polystyrene beads (mean diameter 250 nm) was added to the slides. After the beads were immobilized on the coverslip, Cy5-labeled NeutrAvidin was added, which bound to the beads via biotin. With the right buffer conditions, Cy5 is a switchable fluorescence dye, which is widely used for STORM. Fluorescence imaging was performed on a Nikon N-STORM system. The acquisition was performed using dSTORM (direct STORM). The buffer was PBS with 100mM

mercaptoethylamine, 5% Glucose, 0,5 mg/ml Glucose Oxidase and 40 μg/ml Catalase. A high power 647 nm laser was used for switching the fluorophores to a stable dark state and for readout. Additional photo-switching to the on-state was accomplished using a 405nm activation laser, when required. STORM data were analyzed in Nikon's NIS-elements imaging software. The result is shown in Figure 2. It can be seen how the optical resolution is increased by using STORM. Furthermore, AFM data can be recorded on the same position with high accuracy. While it is impossible to distinguish between single or multiple bead sets in the conventional fluorescence image, it is possible to do so by STORM and AFM. The STORM image furthermore clearly shows that the fluorescence dyes are located on the surface of the single beads. Just a conjugation of three beads, which are very close to each other, cannot be resolved perfectly in STORM. Here, AFM was taken

to have an optimal resolution of these set of three beads. The AFM image furthermore provides a high resolution 3-dimensional topography image. A cross section of the single beads can be used to define the correct height of the used beads of about 250 nm.

## Application example 2: HeLa cells

In a second example HeLa cells were investigated. The HeLa cell line is a commonly used human cell line which was harvested from cervical cancer cells. The used HeLa cells were grown on coverslips to about 50% confluency and then fixed with formaldehyde. The microtubules were labeled via immuno-fluorescence. Therefore, mouse anti-alpha-tubulin antibody was used as a primary antibody. Alexa647-labeled anti-mouse antibody was used later on as secondary antibody for the fluorescence staining. Alexa647 is widely used as a switchable fluorescence dye for STORM [12]. It has an excitation wavelength of 650 nm, an emission of 665 nm. STORM imaging was performed as for the labeled beads. Figure 6 demonstrates the results of the STORM and AFM measurements. The individual microtubular structures can be easily resolved with STORM. The AFM height image and especially the overlay image of STORM and AFM provide further information about the cell surface appearance with respect to the microtubules and their distribution. Also the mechanical properties were investigated to complete the picture of the measured HeLa cell. Therefore JPK's Quantitative Imaging (QI™) mode was used [13]. This newly developed AFM mode provides high resolution imaging and high resolution mechanical measurements in parallel [14][15]. On each pixel a full force distance curve is recorded to obtain next to a height also e.g. adhesion and elasticity images.

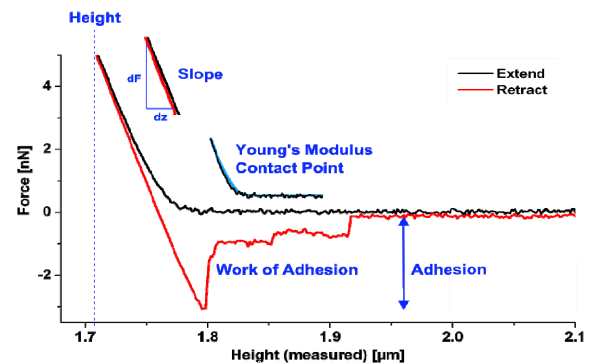


Figure 7: Principle of QI™ mode and possible information that can be obtained out of a force distance curve.

The basic approach is to use a force spectroscopy based vertical movement. This prevents the application of any lateral forces. Furthermore, the interaction force between tip and surface is controlled and defined at every time. The newly-developed tip movement algorithm and the high sampling rate of 800 kHz make a fast data acquisition possible. To measure controlled force distance curves (FD-curve) it is ensured that no x, y movement takes place while the FD-curve is recorded and that there is a constant velocity in approach and retract [16]. (For further information see application note: [“QI™ mode - Quantitative Imaging with the NanoWizard® 3 AFM”](#)). The recorded force distance curves are saved and can be analyzed offline in a user-defined manner. Here it is possible to have a closer look into the data to calculate e.g. the Young's modulus or to identify recognition events. For a fast and convenient analysis the fully automated batch processing tool can be used. In batch processing all recorded FD-curves can be analyzed automatically in the same way and a batch of different operations can be applied. The results can be displayed as an image and a histogram. Figure 6 E-G) shows different nanomechanical information. The adhesion image provides information about a maximal unbinding force or stickiness of the sample. As expected, the cells show a higher adhesion than the non-treated coverslip substrate. Also elasticity information is in the spotlight of cell and material research [17][18]. Especially in the fields of cancer and

development biology it is possible to correlate changes in the nanomechanical appearance with functional changes. To get quantitative data, the Young's Modulus was calculated with the well-established Hertz fit. Here, it is possible to use different types of indenter geometries and adjust fitting parameter like the indentation depth. As a result of the Hertz fit the Young's modulus as well as the contact point can be assigned. The result of the Young's modulus is displayed in figure 6G. The surface of the cell shows an inhomogeneity of the Young's modulus which cannot be directly correlated to the microtubular structures. In further investigations it could be interesting to stain actin filaments as well or to investigate different cell lines with different cytoskeleton characteristics to compare the results. As already mentioned, the contact point is additional information derived from the Hertz fit. The contact point is the height at which the cantilever just starts to touch and indent the surface. The Contact Point Imaging (CPI) demonstrated therefore the surface at zero interaction force, which is totally new in AFM research. In all other AFM measurement methods it is only possible to get information about the surface at a chosen interaction force. Contact Point Imaging offers a new perspective especially on soft sample like cells (For further information see application note: "Investigations on living cells using JPK's QI™ mode"). Figure 8 demonstrates the height image at 1 nN force and the contact point image at zero force.

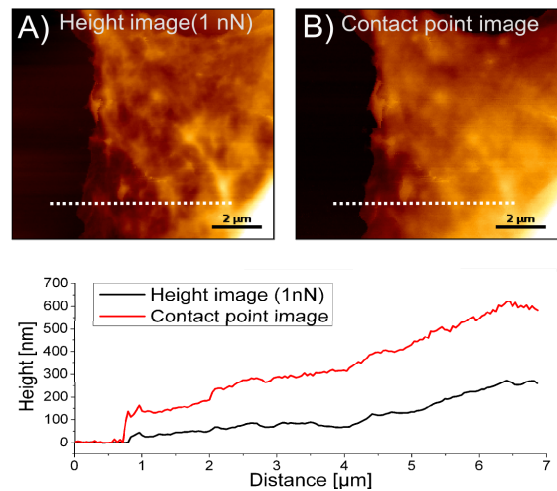
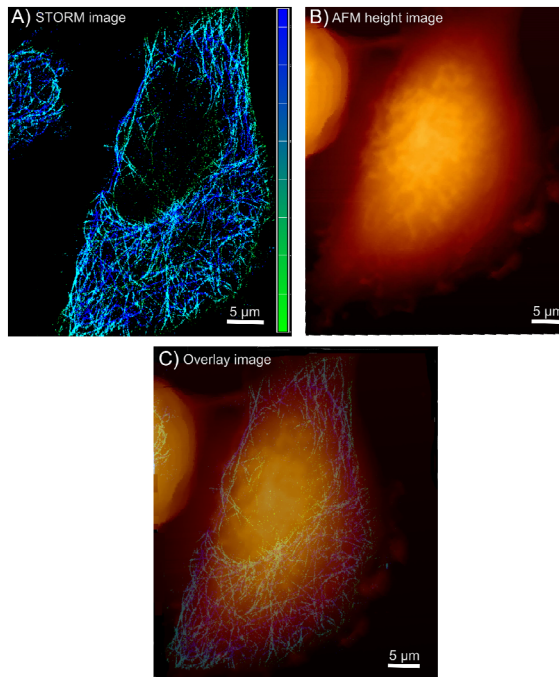


Figure 8: Height and contact point image of HeLa cell. The dotted line corresponds to the cross section which is displays in the diagram below.

It can be clearly seen that the HeLa cell in the contact point image has a smoother membrane structure. The membrane and cytoskeleton features are much more prominent in the height image. The big effect of the interaction force can be identified even stronger in the displayed cross sections. The same cell region was chosen and it can be recognized that the interaction force of 1 nN leads to a compression of the cell surface of 100 to 400 nm. Especially in the softer cell region a strong compression can be detected. This underlines that QI™ can be used to investigate the influence of external forces on the surface or for AFM tomography measurements [19].

In a second step also whole HeLa cells were investigated to demonstrate the possibility of a combination of 3D STORM and AFM (figure 9). This feature enlarges the benefits of a combination due to the fact that intracellular structures can be resolved optically in three dimensions, while the surface topography and nanomechanics can be measured simultaneously. In conventional fluorescence imaging the axial resolution is limited due to diffraction (>500 nm). In single-molecule localization based super-resolution it is possible to measure the z-position of a single fluorophore with an accuracy below the diffraction

limit. This can – for example - be achieved by introducing a cylindrical lens into the imaging path. Due to the astigmatism, the image of a single fluorophore shows an ellipticity which is sensitive to the molecules' distance from the focal plane. Analysis of this ellipticity allows determining the position in 3D [20]. In astigmatism-based 3D STORM it is possible to achieve an axial resolution of ~50-75 nm over a z-range of about 800 nm.



*Figure 9: AFM image overlaid with 3D STORM. A) STORM images shows the different microtubular structures in 3D (z-range: -400 nm – 400 nm) B) AFM image of the whole HeLa cell recorded with QI™ mode (z-range: 6 μm) C) Overlay of both images*

Figure 9 demonstrates the 3D STORM image of a HeLa cell. The microtubules distribution and structure can be resolved in a z-range of about 800nm. The AFM image provides the topography information of the whole cell. It has to be pointed out that the measured cell has a height of about 6 μm. The nucleus region is the highest point in the cell body. This region can also be identified in the STORM image, due to the fact that there are no microtubules in this region. The overlay of both pieces of information further underlines this result.

## Conclusion

The research field of combined optical and AFM measurements is nearly unlimited. Especially in life science research this new combination of super-resolution optical microscopy and AFM provides new possibilities. This technical note should offer a first view in the potential of combined experiments, where high resolution optical STORM measurements and high resolution AFM measurements can assist each other in a productive way (For further information concerning a STED and AFM combination see technical note: [“Combining AFM with super-resolution STED \(stimulated emission depletion\) microscopy system”](#)). The nanomechanical measurements which can be provided with QI™ fulfill the investigations and will become more and more important in future studies.

## Acknowledgements

Many thanks to Prof. Römer and the Cluster of Excellence “Centre for Biological Signalling Studies” (BIOSS, University of Freiburg, Germany) for the possibility of using their STORM setup in combination with the JPK NanoWizard 3.

## Authors

Anne Hermsdörfer  
JPK Instruments AG  
Bouchéstraße 12  
12435 Berlin  
Germany  
[hermsdoerfer@jpk.com](mailto:hermsdoerfer@jpk.com)

Dr. Josef Madl and Jun.-Prof. Dr. Winfried Römer  
Albert-Ludwigs University Freiburg  
Institute of Biology II and BIOSS  
Schänzlestraße 18  
79104 Freiburg  
Germany  
[josef.madl@bioss.uni-freiburg.de](mailto:josef.madl@bioss.uni-freiburg.de)  
[winfried.roemer@bioss.uni-freiburg.de](mailto:winfried.roemer@bioss.uni-freiburg.de)

## Literature

- [1] Braga P.C., Ricci, D.: Atomic Force Microscopy: Biomedical Methods and Applications, Hamana Press Inc., Totowa, 2004
- [2] Gadegaard N.: Atomic force microscopy in biology: technology and techniques, Biotechnic & Histochemistry 81: 87-97, 2006
- [3] Tabor, R.F., Lockie, H., Mair, D., Manica, R., Chan, D.Y. C., Grieser, F. Dagastine, R. R.: Combined AFM and Confocal Microscopy of Oil Droplets: Absolute Separations and Forces in Nanofilms, J. Phys. Chem. Letters 2: 961-965 (2011)
- [4] Harke, B., Chacko, J.V., Haschke, H., Canale, C., Diaspro, A.: A novel nanoscopic tool by combining AFM with STED microscopy, Optical Nanoscopy 1 (2012)
- [5] Schermelleh, L., Heintzmann, R., Leonhardt, H.: A guide to super-resolution fluorescence microscopy, J. cell biol. 190: 165-175 (2010)
- [6] Huang, B., Wang, W., Bates, M., Zhuang, X.: Super-resolution fluorescence microscopy, Annu. Rev. Biochem 78: 993-1016 (2009)
- [7] Patterson, G., Davidson, M., Manley, S., Lippincott-Schwartz, J.: Superresolution imaging using single-molecule localization, Annu. Rev. Phys. Chem. 61: 345-267 (2010)
- [8] Silfies, J.S., Schwartz, S.A., Davidson, M.W.: Introduction to Stochastic optical reconstruction microscopy (STORM), Nikon (2013)
- [9] Bates, M., Huang, B., Zhuang, X.: Super-resolution microscopy by nanoscale localization of photo-switchable fluorescent probes, Curr. Opin. Chem. Biol. 12: 505-514 (2008)
- [10] Owen R.J., Heyes C.D., Knebel D., Nienhaus, G. U.: An integrated instrumental setup for the combination of atomic force microscopy with optical spectroscopy, Biopolymers 82: 410-414 (2006)
- [11] Van de Linde, S., Aufmkolk, S., Franke, C., Holm, T., Klein, T., Löschberger, A., Poppert, S., Wolter, S., Sauer, M.: Investigating cellular structures at the nanoscale with organic fluorophores, Chemistry & biology 20: 8-18 (2013)
- [12] Huang, B., Babcock, H., Zhuang, X.: Breaking the diffraction Barrier: super-resolution imaging of cells, Cell 143: 1047-1058 (2010)
- [13] Haschke H., Jähnke T.: Nanometrology-QI™ offers next-generation AFM imaging mode for nanometrology, Laser Focus World, 48, 2012
- [14] M. Horimizu, T. Kawase, T. Tanaka, K. Okuda, M. Nagata, D. M. Burns, H. Yoshie: Biomechanical evaluation by AFM of cultured human cell-multilayered periosteal sheets, Micron, 2013
- [15] L. Chopineta, C. Formosaa, M.P. Rols, R.E. Duval, E. Dague: Imaging living cells surface and quantifying its properties at high resolution using AFM in QI™ mode, Micron, 2013
- [16] Butt, H.-J., Capella, B., Kappl, M.: Force measurements with the atomic force microscope: Technique, interpretation and applications, Surface Science Reports 59: 1-152, 2005
- [17] Harris A.R., Charras G. T.: Experimental validation of atomic force microscopy-based cell elasticity measurements, Nanotechnology 22 (2011)
- [18] Zahn, J.T., Louban, I. Jungbauer, S., Bissinger, M. Kaufmann, D., Kemkemer, R. Spatz, J. P.: Age-Dependent Changes in Microscale Stiffness and Mechanoresponses of Cells, Small 7:1480-1487 (2011)
- [19] Longo G., Rio L. M., Roduit C., Trampuz A., Bizzini A., Dietler G., Kasas S.: Force volume and stiffness tomography investigation on the dynamics of stiff material under bacterial membranes, J. Mol. Recognit. 25: 278-284, 2012
- [20] Huang, B., Wang, W., Bates, M., Zhuang, X.: Three-dimensional super-resolution imaging by stochastic optical reconstruction microscopy, Science 319:810-813 (2008)